

ChemComm

Accepted Manuscript



This is an *Accepted Manuscript*, which has been through the Royal Society of Chemistry peer review process and has been accepted for publication.

Accepted Manuscripts are published online shortly after acceptance, before technical editing, formatting and proof reading. Using this free service, authors can make their results available to the community, in citable form, before we publish the edited article. We will replace this *Accepted Manuscript* with the edited and formatted *Advance Article* as soon as it is available.

You can find more information about *Accepted Manuscripts* in the [Information for Authors](#).

Please note that technical editing may introduce minor changes to the text and/or graphics, which may alter content. The journal's standard [Terms & Conditions](#) and the [Ethical guidelines](#) still apply. In no event shall the Royal Society of Chemistry be held responsible for any errors or omissions in this *Accepted Manuscript* or any consequences arising from the use of any information it contains.

Micromotor-based On-Off Fluorescence Detection of Sarin and Soman Simulants

Cite this: DOI: 10.1039/x0xx00000x

Received 00th January 20xx,
Accepted 00th January 20xx

DOI: 10.1039/x0xx00000x
www.rsc.org/

Virendra V. Singh, Kevin Kaufmann, Jahir Orozco, Jinxing Li, Michael Galarnyk,

Guarav Arya, Joseph Wang*

Self-propelled micromotor-based fluorescent “On-Off” detection of nerve agents is described. The motion-based assay utilizes Si/Pt Janus micromotors coated with fluoresceinamine toward real-time “on-the-fly” field detection of sarin and soman simulants.

Chemical warfare agents (CWA) are some of the most nefarious weapons of mass destruction.^[1] The ease of manufacturing and dispensability, ease of availability, and inexpensive starting materials make them an eminent global threat.^[1] Nerve agents are a particularly dangerous class of CWA that continue to be a threat in spite of controls imposed by the Chemical Weapon Convention (CWC) which prohibits the production and use of chemicals on enemy forces.^[2,3] Their rapid and severe effects on human health stem from their ability to irreversibly inhibit acetylcholinesterase activity by phosphorylation and leads to neuromuscular paralysis and eventually death.^[4-6] A particularly dangerous class of organophosphorus nerve agents is the phosphoryl fluoride containing species such as sarin and soman^[7-9], referred to as GB and GD agents, respectively. Unfortunately, these highly reactive and volatile nerve agents are colorless, odorless, and tasteless, making their detection very difficult. Therefore, a reliable and rapid nerve agent detection system is highly desirable amidst the current climate of terrorism awareness. Among a variety of detection methods that have been developed for these nerve agents,^[9] fluorescent detection offers the unrivaled merits of high sensitivity, low-cost and operational simplicity.^[10-12] The chromo-fluorogenic detection is especially attractive because it allows simple visual detection *in situ*, or on-site, without any sample pretreatment or the use of complex equipment.^[10-12] As a result, the development of highly sensitive, selective, ready-to-use, and rapid field screening methods for these nerve agents has become an increasingly imperative research goal. Herein we demonstrate an extremely fast (~10 sec) fluorescent “On-Off” detection of sarin and soman simulants based on self-propelled dye-coated micromotors. Artificial/synthetic micromotors have recently attracted considerable interest due to their attractive capabilities and diverse potential applications, ranging from directed drug delivery to environmental detection.^[13-15] The self-propulsion capability of micromotors induces efficient fluid mixing, a very useful property for environments that would not allow mechanical agitation (i.e., bodies of water, stealthy national defense operations, etc.) or at the microscale level. This motor-induced mixing has shown to be extremely effective in accelerating both target-receptor interaction,^[13-15] detection,^[16,17] and detoxification reactions.^[18-20]

Recently, there has been a considerable interest in micromotor-based defenses against chemical and biological warfare agents^[18-20], these include the potential use of functionalized micromotors as efficient screening tools for the real time and on-site detection of chemical threats in environmental matrices.

Fluorescence quenching methods have been emerging as effective route for sensitive and low cost field detection.^[21-23] In this regard, fluorescent ‘turn-off’ based sensors have been developed for nitrated explosive compounds^[22] and Hg²⁺^[23]. Such ‘turn-off’ sensors have shown to be more sensitive than their ‘turn-on’ sensor counterpart.^[22-23] The motion-based accelerated nerve-agent detection, described in the present work and illustrated in Figure 1, relies on coating a catalytic microsphere micromotors with the fluorophore fluoresceinamine (FLA) that reacts quickly with phosphoryl halides.^[24] Diethyl chlorophosphate (DCP) is used as a nerve agent simulant as it has similar reactivity of common nerve agents, yet lacks their potent efficacy and related safety concerns.^[12] Sarin and soman possess highly reactive fluorine groups that inhibit acetylcholinesterase by covalent modification of its active site. In this work, this property of these nerve agents was exploited using DCP as a nerve agent simulant for its reactive chlorine group (Figure S1). DCP has been selected because it has a labile -Cl group, similar to the reactive -F group of sarin and soman. The -NH₂ group of the FLA dye will react with the phosphoryl group of reactive CWA simulant only due to the presence of reactive (Cl or F) group. In the case of non-reactive simulant phosphoryl moiety, such as DMMP, no such labile reactive group is available which restrict the reaction with the -NH₂ group of dye, making the process specific to reactive nerve agents.

Microbead chemical switches were shown useful for detecting reactive organophosphate CWA vapors using buffers and appropriate proton scavengers.^[25] Moreover, it was also found that fluorescence intensity increased first and then decreased over time which may lead to false positive fluorescent “Off-On” detection. However, since in the field conditions, including the concentration of CWA and other metrological conditions are often unknown, the detection of CWA in natural water matrices is more challenging compared to vapor measurements since proper buffering and a suitable proton scavenger are very important. To date, this has made the detection process unfeasible. As will be illustrated below, the new micromotor strategy addresses these challenges toward rapid fluorescent “On-Off” route for instantaneous detection of sarin and soman simulants.

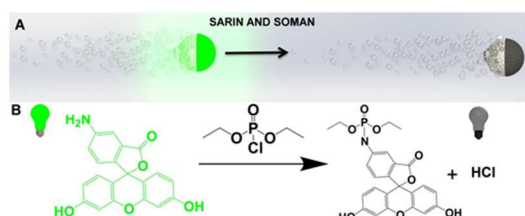


Figure 1. Schematic representation of the micromotor based ‘on-the-fly’ fluorescent “On-Off” detection of nerve agent and (B) reaction mechanism showing the reaction of FLA coated micromotor with DCP.

The self-propulsion capability of the dye-coated micromotors, along with the corresponding bubble tail, are shown to generate effective fluid convection (without external force) that results in an increased rate of collision between the micromotors and the target nerve agent, thereby offering a rapid ‘on-the-fly’ fluorescent “On-Off” detection method. The fluid mixing capability of micromotors^[26] has been used recently for accelerated environmental remediation and detoxification processes.^[18-20] Similarly, the efficient movement of the FLA-coated microsphere, along with the substantial fluid transport, are used in the following sections for developing an attractive “On-Off” CWA detection approach.

As illustrated in Fig.1A, self-propelled FLA/Silica-NH₂/Pt micromotors perform “on-the-fly” fluorescent detection of nerve agents in environmental matrices. Figure 1B displays the reaction mechanism involved the FLA/Silica-NH₂/Pt micromotor and nerve agent. These micromotors, along with inherent efficient solution mixing, resulted in the dramatic quenching of FLA fluorescence upon encountering nerve agents in solution.

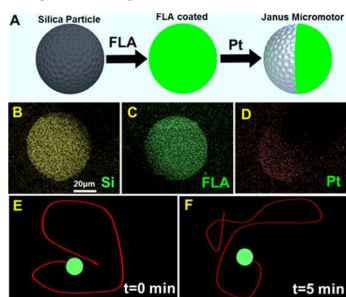


Figure 2. (A) Schematic detailing the fabrication steps in the preparation of FLA/silica-NH₂/Pt micromotors; (B, C, D) energy-dispersive X-ray (EDX) spectroscopy images illustrating the distribution of Si, dye and Pt; (E) Tracking line (taken from Supporting information video S1) illustrating the typical trajectories traveled by a micromotor over 5 second intervals at (E) t=0min and (F) t=5min.

Figure 2A illustrates the fabrication steps involved in the preparation of FLA/Silica-NH₂/Pt micromotors for the detection of nerve agents. The new micromotors were prepared by impregnation of FLA into silica microparticles using the incipient wetness technique^[27] (refer to experimental section) followed by asymmetric deposition (for the dynamic movement of micromotors) of Pt by sputtering (Fig. 2A). This technique allows the FLA solution to just wet the adsorbent and be completely adsorbed on solid silica-NH₂ particles.

Scanning electron microscopy (SEM) images of silica-NH₂ particle before and after the dye loading are shown in the Supporting Information. The surface of FLA coated silica particles displays a rough, shiny, and bright white morphology when compared to unmodified silica particles, indicating that the FLA molecules are adsorbed on the surface of silica-NH₂ microparticles. Energy dispersive spectroscopic (EDX) analysis of impregnated and un-

impregnated samples qualitatively confirms the impregnation as indicated by the presence of the respective element in the EDX spectra (refer to Supporting Information). The presence of Janus micromotors is also confirmed by the corresponding EDX mapping of Pt and carbon displayed in Fig. 2C-D. Fig. 2E and F illustrate the initial movement of the dye coated micromotors in pure water and the movement after 5 minute propulsion, respectively. The tracking trajectories in Fig. 2 E and F display the motion over a 5 s period, with an average speed of ~145 μm/s.

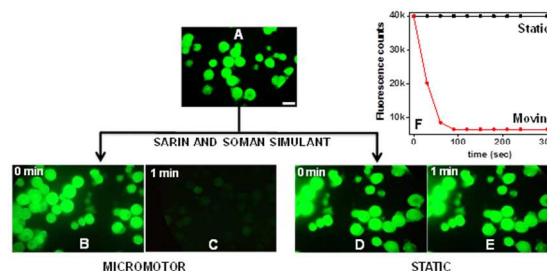


Figure 3. (A) Fluorescent intensity of FLA coated silica-NH₂ particles; (B) Fluorescent intensity of FLA/silica-NH₂/Pt micromotors before exposure to DCP; (C) after exposure; (D) Fluorescent intensity of FLA/silica-NH₂/Pt static particles before exposure of DCP; (E) after exposure; and (F) graph showing the movement of micromotors leading to rapid quenching of fluorescence compared to static. Reaction conditions: conc. of DCP = 10⁻³M, H₂O₂ (2%), SDS (1%), and 2×10⁴micromotors; λ_{ex}, 490 nm; λ_{em}, 510 nm. Scale bar 45μm.

To demonstrate the practical utility of the new micromotor-based fluorescent “On-Off” nerve-agent detection in environmental matrices, we investigated the ability to detect the sarin and soman simulants (Figure S1). In order to mimic the natural environment, all experiments were carried out in water without buffer for the real time detection of nerve agents. Figure 3 shows a FLA-coated silica-NH₂ particle that exhibits fluorescence counts of ~40,000. Fig. 3B and C displays the comparative fluorescence intensity before and after FLA/Silica-NH₂/Pt micromotors navigated a DCP contaminated solution (10⁻³ M), respectively. There is an instant fluorescence quenching of the moving micromotor compared to static particles that did not show any fluorescence quenching under the same conditions, even after 5 min of interaction (Figure 3D and E). Figure 3F shows the crucial role of the movement of micromotors in the contaminated solution for the rapid screening of nerve agents when compared to the static coated particles under similar conditions. The unique movement of multiple micromotors with bubble generation across the contaminated samples results in a continuous mixing (without external agitation), which increases the likelihood of collision with nerve agent and leads to an increase in the rate of reaction, with the concomitant fluorescence quenching within a minute, as per collision theory.^[28] This dramatic fluorescence quenching is attributed to the reaction of reactive phosphonates with the –NH₂ group of dye-coated micromotors which leads to the respective phosphoramidate while releasing HCl which causes the interruption of the fluorophore’s conjugation.^[29] Unlike the fluorescence intensity increase expected from the formation of phosphoramidate,^[25] we observed a dramatic quenching in the fluorescence intensity of the FLPA adduct, attributed to the local decrease in pH due to the HCl release.

In contrast, when we performed the experiments in buffered solutions the fluorescence intensity was shown to increase initially. However, at higher concentrations of nerve agent the fluorescence intensity decreased over the same time period, due to insufficient buffer capacity. Nevertheless, since in the field conditions including

the concentration of CWA and other metrological conditions are unknown, buffering of the solution is a very challenging task. Therefore, in real field conditions, it is possible to have false positive fluorescent “Off-On” detection without proper buffering. Yet, towards the development of a screening method that rapidly alerts the presence of CWA in field conditions, we have adopted the micromotor-based ‘on-the-fly’ fluorescent instantaneous CWA detection in un-buffered solutions. The fluorescence quenching time can be related to the concentration of CWA. Additional semi-quantitative information based on the increase of fluorescence intensity of the FLPA adduct can be achieved in a buffered solution with careful pH control and a proper acid scavenger.

To expand the practical utility of the dye-coated micromotors towards diverse environmental applications, the fluorescence intensity of micromotors were also tested in sea water, pool water, and lake water. The resultant fluorescence intensity profile was consistent with that found in water experiments, which reflects its applicability in diverse natural environments. The specificity of this micromotor based detection was confirmed by monitoring the fluorescence with non-reactive phosphonates, such as dimethyl methyl phosphonate (DMMP; 10^{-3} M), and no fluorescence change was observed. The efficiency of the new micromotor-based *on-the-fly* fluorescent “On-Off” detection strongly depends on the concentration of nerve agents. Figure 4A displays the time dependent quenching of FLA-coated micromotors with respect to varying DCP concentrations ranging from 10^{-1} to 10^{-6} M using a fixed number of micromotors. As expected, the fluorescence quenching is very fast (within a minute) for concentrations as low as 10^{-3} M DCP. Moreover, this micromotors based detection platform is able to sense concentrations as low as 10^{-6} M DCP within 3 minutes. The detection efficiency at different concentrations of DCP with micromotor and static dye-coated particles was also compared (Fig. 4B). As expected, the reaction between the FLA-coated micromotors and the target DCP was very fast. For example, quenching of the motors was observed after only 120 s of interaction with a 10^{-4} M DCP contaminated solution. In contrast, when the contaminated solution is in quiescent conditions, the reaction between static FLA-coated silica particles and DCP is inefficient, thereby requiring around 30 min to exhibit a quenching of the fluorescence.

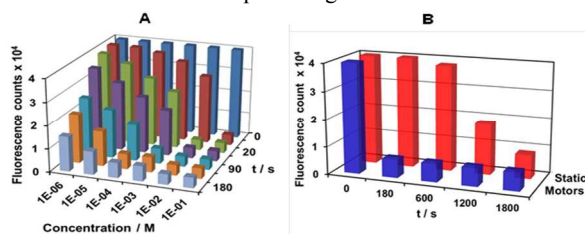


Figure 4. Effect of inter-dependent parameters on the quenching of fluorescence intensity of FLA/Silica-NH₂/Pt micromotors: (A) Time dependent quenching of micromotors with different concentrations of DCP; and (B) comparison of fluorescent quenching with micromotor and static FLA-coated silica with 10^{-4} M DCP. Reaction conditions: H₂O₂ (2%), SDS (1%), λ_{ex} , 490 nm; λ_{em} , 510 nm.

In order to optimize the density of micromotors for the rapid detection of 10^{-6} M DCP solution, different numbers of FLA-coated silica micromotors (1×10^4 to 2×10^4 micromotors/ml), were propelled in 600 μ l contaminated solution for 3 min. It was found that an increase in the micromotor density increases the rate of CWA detection. Figure S4 displays the effect of micromotor density on the detection rate (rapid fluorescence quenching) of DCP in a contaminated solution. We have also performed micromotor-based fluorescent enhancement detection of DCP in a phosphate buffer (pH 7.2) medium based on the conversion of dye in to phosphoramidate.

This resulted in a rapid and intense initial fluorescence increase in the presence of different DCP concentrations (Fig. S5). However, this data illustrates that at longer times (>1.5 min) this enhancement may decay, depending on the DCP concentration. Such decrease is expected for this specific phosphoramidate reaction since there is also a release of hydrochloric acid which can be partially neutralized by the buffer medium. At higher DCCP concentrations ($>10^{-2}$ M), more acid production results in fluorescence quenching after the initial increase which may lead to false positive alarms. Accordingly, practical detection applications based on the fluorescence enhancement should rely on the initial response in the buffer medium over the first 90 sec. Figure S6 shows the crucial role of the movement of micromotors in the buffer solution (pH 7.2) containing 10^{-3} M of DCP, compared to the static dye-coated particles under similar conditions. As expected, the fluorescence intensity drastically increases when compared to the static counterpart, reflecting the near instantaneous reaction of DCP with dye-coated micromotors due to continuous mixing associated with the micromotor movement. So, in both cases (buffer or non-buffer media) the micromotors lead to a greatly enhanced sensitivity compared to static systems. Interference studies were carried out in the presence of common volatile organic compounds, including ethanol, toluene, acetone, and isopropanol in order to demonstrate the applicability of the present methodology. As illustrated in Figure S7, these organic compounds had a negligible effect upon the fluorescent signal, indicating effective discrimination against volatile organic compounds.

The greatly enhanced detection reflects the fluid mixing capability of the dye-coated micromotors. The experimentally observed rapid fluorescent detection achieved by the mobile micromotors, compared to static micromotors, can be attributed to and explained mathematically by three effects. First, the propulsion of mobile motors is able to keep them suspended and well dispersed in the solution. In contrast, the static motors settle to the bottom of the container, due to gravity, forming a densely packed aggregate. The mass-transfer model for the two systems provided in the Supplementary Information shows that motors well dispersed in solution lead to significantly smaller diffusion mass-transfer resistance compared to sedimented motors; even without accounting for the continuous movement of the micromotors. This model estimates an enhancement of roughly $1 + (\pi Dt/4R^2)^{1/2}$ in the amount of analyte (DCP) reacted after time t at the surface of dispersed versus sedimented motors, where D is the diffusivity of the analyte in solution, R is the motor radius, and t is the time. Plugging in our determined estimates of DCP diffusivity and our micromotor size, one obtains a possible experimental enhancement due to micromotor suspension up to 25-fold during the first 10 minutes of motor activity. Second, the motion of the micromotors leads to convection-induced enhancement in the mass transfer of the analyte. In other words, the mobile motor leads to a larger number of collisions between the analyte and the motor surface, thereby enhancing the net rate of reaction. It can be shown that the additional enhancement in the flux arising from motor motion, on top of diffusion, is roughly given by $\sim 0.664 Re^{1/2} Sc^{1/3}$, where Re is the Reynolds number and Sc is the Schmidt number. Our calculations find this additional enhancement due to convection to be $\sim 31\%$ more than diffusion alone (see Supplementary Information). Third, the continuous formation of bubbles during motor propulsion leads to improved mixing of the analyte in the solution, which is also expected to increase the transport of analyte to the surface of the motors. While the 44 fold-enhancement in surface flux due to this effect is difficult to estimate, we have previously shown that the generated bubbles significantly enhance the transport of tracer particles in the vicinity of the motors.^[26] Thus, the combined effects of the propulsion of

micromotors are critical to the rapid detection of the target analyte whereas static lead to slow rates of reaction and long operation time.^[30] Similar enhancements in mass transport have been observed in other self-propelled systems.^[18-20,30,31]

Conclusions

In conclusion, we have demonstrated the first example of a micromotor based fluorescent “On-Off” strategy for the rapid ‘on-the-fly’ screening of sarin and soman related threats within seconds. The continuous mixing induced by the motion of multiple micromotors across a contaminated sample results in a greatly enhanced mass transport, and hence leads to increased rates of reaction between contaminated solution and micromotors when compared to static micromotor counterparts. The rapid micromotors based screening can be coupled to more elaborate fluorescence enhancement strategies to confirm nerve agent presence. The same reaction has also been performed in a buffer medium where the presence of the dye-coated micromotors led to a significantly pronounced response compared to static parts. Compared to common nerve agent detection methodologies, this micromotor-based screening methodology gives real time detection towards on-site measurements in many environmental matrices. Movement of the FLA-coated micromotors accelerates their “on the fly” real-time quenching of fluorescence upon contact with reactive nerve agents. The present study thus supports that the motion of micro/nanoscale motors and the corresponding fluid transport can notably improve the rapid and reliable detection of sarin and soman. We anticipate that the present micromotor-based fluorescent detection platform can be implemented practically and inspire further research in the field of micromotor-based sensing towards a broad range of chemical threats. The autonomous movement and built-in fluid mixing capability of dye-coated micromotors thus hold considerable promise for enhancing the detection power of a wide range of chemical sensing processes.

Acknowledgements

This project received support from the Defense Threat Reduction Agency-Joint Science and Technology Office for Chemical and Biological Defense (Grant no. HDTRA1-13-1-0002) and the UCSD Calit2 Strategic Research Opportunities (CSRO) program.

Notes and references

Department of Nanoengineering, University of California San Diego, La Jolla, CA 92093 (USA)

*Correspondence to: josephwang@ucsd.edu

1. Y. C. Yang, *Acc. Chem. Res.*, 1999, **32**, 109-115.
2. W. Krutzsch, R. Trapp, *In: A commentary on the chemical weapons convention*. London: MartinusNijhoff Publishers; 1994.
3. Organization for the Prohibition of Chemical Weapons. Proceedings, Convention on the Prohibition of the Development, Production, Stockpiling and Use of Chemical Weapons and on Their Destruction; Opened for Signature: Paris, France, 1993.
4. M. Ehrlich, in *Encyclopedia of Toxicology*, ed. P. Wexler, Academic Press, San Diego, CA, 1998, p. 467.
5. F. R. Sidell, J. Borak, *Ann. Emerg. Med.*, 1992, **21**, 865-871.
6. T. C. Marrs, *Pharmacol. Ther.*, 1993, **58**, 51-66.
7. S. E. Letant, M. J. Sailor, *Adv. Mater.*, 2000, **12**, 355-359.
8. S.W. Zhang, T. Swager, *J. Am. Chem. Soc.*, 2003, **125**, 3420-3421.
9. a) H. Sohn, S. E. Letant, M. J. Sailor, W. Trogler, *J. Am. Chem. Soc.*, 2000, **122**, 5399-5400; b) J. Wang, M. Pumera, G.

- E. Collins, A. Mulchandani, *Anal. Chem.*, 2002, **74**, 6121–6125; (c) S. Jo, D. Kim, S. H. Son, Y. Kim, T.S. Lee, *ACS Appl. Mater. Interfaces* 2014, **6**, 1330–1336; (d) J. Lee, S. Seo, J. Kim, *Adv. Funct. Mater.* 2012, **22**, 1632–1638.
10. A. Barba-Bon, A. M. Costero, S. Gil, F. Sancenon, R. Martinez-Manez, *Chem. Commun.*, 2014, **50**, 13289-13291.
11. S. Han, Z. Xue, Z. Wang, T. B. Wen, *Chem. Commun.*, 2010, **46**, 8413-8415.
12. T.J. Dale, J.Rebek Jr., *J. Am. Chem. Soc.*, 2006, **128**, 4500-4501.
13. D. Patra, S. Sengupta, W. Duan, H. Zhang, R. Pavlick, A. Sen, *Nanoscale*, 2013, **5**, 1273–1283.
14. W. Gao, X. Feng, A. Pei, Y. Gu, J. Li, J. Wang, *Nanoscale*, 2013, **5**, 4696–4700.
15. E. Morales-Narváez, M. Guix, M. Medina-Sánchez, C. C. Mayorga-Martinez, A. Merkoçi, *Small*, 2014, **10**, 2542–2548.
16. W. Gao, J. Wang, *ACS nano*, 2014, **8**, 3170-3180.
17. a) D. Kagan, S. Campuzano, S. Balasubramanian, F. Kuralay, G. Flechsig, J. Wang, *Nano Lett.*, 2011, **11**, 2083–2087; b) J. G. S. Moo, H. Wang, G. Zhao, M. Pumera, *Chem. Eur. J.*, 2014, **20**, 4292–4296.
18. J. Orozco, G. Cheng, D. Vilela, S. Sattayasamitsathit, R. Vazquez-Duhalt, G. Valdes-Ramirez, O. S. Pak, A. Escarpa, C. Kan, J. Wang, *Angew. Chem. Int. Ed.*, 2013, **52**, 13276-13279.
19. a) J. Li, V. V. Singh, S. Sattayasamitsathit, J. Orozco, K. Kaufmann, R. Dong, W. Gao, B. Jurado-Sanchez, Y. Fedorak, J. Wang, *ACS Nano*, 2014, **8**, 11118-11125; b) V. V. Singh, B. Jurado-Sánchez, S. Sattayasamitsathit, J. Orozco, J. Li, M. Galarnyk, Y. Fedorak J. Wang, *Adv. Funct. Mater.*, 2015, **25**, 2147–2155.
20. B. Jurado-Sanchez, S. Sattayasamitsathit, W. Gao, L. Santos, Y. Fedorak, V. V. Singh, J. Orozco, M. Galarnyk, J. Wang, *Small*, 2015, **11**, 499-506.
21. C. J. Cumming, C. Aker, M. Fisher, M. Fox, M. J. Grone, D. Reust, M. G. Rockley, T. M. Swager, E. Tower, V. William, *IEEE Trans. Geosci. Remote Sens.*, 2001, **39**, 1119-1128.
22. A. Rana, P. K. Panda, *RSC Adv.*, 2012, **2**, 12164–12168.
23. J. Du, M. Liu, X. Lou, T. Zhao, Z. Wang, Y. Xue, J. Zhao, Y. Xu, *Anal. Chem.*, 2012, **84**, 8060–8066.
24. a) L. A. Saari, W. R. Seitz, *Anal. Chem.* 1982, **54**, 821–823; b) Z. Zhang, Y. Zhang, W. Ma, R. Russell, Z. M. Shakhsher, C. L. Grant, W. R. Seitz, D. C. Sundberg, *Anal. Chem.*, 1989, **61**, 202–205; c) H. D. Duong, O. J. Sohn, H. T. Lam, J. I. Rhee, *Microchem. J.*, 2006, **84**, 50–55.
25. S. B. Nagale, T. Sternfeld, D. R. Walt, *J. Am. Chem. Soc.*, 2006, **128**, 5041-5048.
26. J. Orozco, B. Jurado-Sánchez, G. Wagner, W. Gao, R. Vazquez-Duhalt, S. Sattayasamitsathit, M. Galarnyk, A. Cortes, D. Saintillan, J. Wang, *Langmuir*, 2014, **30**, 5082–5087.
27. A. Saxena, A. K. Srivastava, B. Singh, A. Goyal, *J. Hazard. Mater.*, 2012, **211**, 226–232.
28. A. K. Dutt, S. C. Miller, *J. Phys. Chem.*, 1993, **97**, 10059-10063.
29. L. Y. Ma, H. Y. Wang, H. Xie, L. X. Xu, *Spectrochim. Acta Part A*, 2004, **60**, 1865–1872.
30. P. Garstecki, M. A. Fischbach, G. M. Whitesides, *Appl. Phys. Lett.*, 2005, **86**, 244108-244110.
31. G. Mico, T. E. Mallouk, T. Darnige, M. Hoyos, J. Dauchet, R. Soto, Y. Wang, A. Rousselet, E. Clement, *Phys. Rev. Lett.*, 2011, **106**, 048102-048104.